Thermal effects in the shear-transformation-zone theory of amorphous plasticity: Comparisons to metallic glass data

M. L. Falk

Department of Materials Science and Engineering, University of Michigan, Ann Arbor, Michigan 48109-2136, USA

J. S. Langer and L. Pechenik

Department of Physics, University of California, Santa Barbara, California 93106-9530, USA

We extend our earlier shear-transformation-zone theory of amorphous plasticity to include the effects of thermally assisted molecular rearrangements. This version of our theory is a substantial revision and generalization of conventional theories of flow in noncrystalline solids. As in our earlier work, it predicts a dynamic transition between jammed and flowing states at a yield stress. Below that yield stress, it now describes thermally assisted creep. We show that this theory accounts for the experimentally observed strain-rate dependence of the viscosity of metallic glasses, and that it also captures many of the details of the transient stress-strain behavior of those materials during loading. In particular, it explains the apparent onset of superplasticity at sufficiently high stress as a transition between creep at low stresses and plastic flow near the yield stress. We also argue that there are internal inconsistencies in the conventional theories of these deformation processes, and suggest ways in which further experimentation as well as theoretical analysis may lead to better understanding of a broad range of nonequilibrium phenomena.

I. INTRODUCTION

In the first paper of this series [1], we showed that energetic constraints determine the principal ingredients of a shear-transformation-zone (STZ) theory of amorphous plasticity. That analysis pertained strictly to the behavior of noncrystalline solids well below their glass temperatures. We turn our attention here to the roles played by thermal fluctuations, specifically, to the ways in which glassy materials make transitions from thermally activated creep to viscoplastic flow near yield stresses.

The atomic mechanisms of plastic deformation are most often described as arising from dislocation motion. This picture breaks down in amorphous solids in which the dislocation, being a lattice defect, ceases to provide a useful description of the microstructural dynamics. In this paper, we describe further progress in the shear-transformation-zone theory of amorphous plasticity that we originally constructed to relate plastic deformation to specific microstructural degrees of freedom in noncrystalline solids. From its inception, our STZ picture has been based on the ideas of Cohen, Turnbull, Spaepen, Argon, and others [2–5], who postulated that plastic deformation in amorphous materials occurs at localized sites usually called flow defects. A number of computational studies (e.g. Refs. [6,7]) have provided support for the idea that a model based on localized defects can capture the dynamics of deformation in such systems. The basic premise of our version of the STZ theory is that these defects must be dynamic entities that carry orientational information; and our most striking conclusion is that, once these orientational degrees of freedom are taken into account, the system so described exhibits an exchange of dynamic stability between jammed and flowing states at a stress that we identify as a yield stress.

Earlier defect theories of deformation in glassy materials appear to us to be incomplete in important respects and, in some cases, to contain physically unrealistic assumptions. These theories generally start by assuming that the plastic strain rate $\dot{\epsilon}^{pl}$ is the product of the density of defects n times an Eyring rate factor [8]:

$$\dot{\epsilon}^{pl} = 2n\nu \, \exp\left(-\frac{\Delta G}{k_B T}\right) \sinh\left(\frac{\Omega \, s}{2k_B T}\right), \qquad (1.1)$$

where ν is a molecular vibration frequency, ΔG is an activation barrier, k_B is Boltzmann's constant, T is the temperature, Ω is an atomic volume, and s is the deviatoric stress (i.e., the shear stress). The authors of these theories then attempt to describe the deformation dynamics by postulating equations of motion for n. The most common choice for such an equation of motion has the form

$$\dot{n} = -k_r n(n - n_{eq}) + P(\dot{\epsilon}^{pl}). \qquad (1.2)$$

Here, k_r is a thermally activated rate factor, n_{eq} is the thermal equilibrium density of flow defects in the absence of external driving forces, and P is a production rate that vanishes when the strain rate is zero. An important example of the use of this equation is the paper by De Hey *et al.* [9]. As we shall see, our STZ theory has many features in common with Eq. (1.2); indeed, some form of each of the terms in this equation will appear here.

There are important differences, however. Theories based on Eqs. (1.1) and (1.3) make no attempt to describe what actually happens when a zone undergoes a shear transformation. Despite the fact that the Eyring formula in Eq. (1.1) describes the balance between forward and backward transitions in some kind of two-state system, the dynamics of atomic scale structural rearrangements described by Eq. (1.1)

     70 011507-1

is decoupled from the population dynamics described by Eq. (1.2). The latter equations therefore implicitly assume that there exists some fast relaxation mechanism—faster than any other rate introduced explicitly in the theory—which causes zones instantaneously to lose their memory of prior transformations.

Another major difference is in the choice of the production function P. In some theories, P is chosen to be linearly proportional to $\dot{\epsilon}^{pl}$, which is impossible because P must be a non-negative scalar while $\dot{\epsilon}^{pl}$ is a tensor that can change sign. Such theories generally are used only in cases where $\dot{\epsilon}^{pl}$ is positive, which may mean that the authors intend to use the magnitude of $\dot{\epsilon}^{pl}$ in more general situations; but the latter convention also would be unsatisfactory because $|\dot{\epsilon}^{pl}|$ is a nonanalytic function that is not likely to arise from any first-principles analysis of molecular mechanisms. In our own earlier paper [10], we tried using the rate of plastic work, $s\,\dot{\epsilon}^{pl}$, in our analog of the production term. That function is a scalar with a satisfactory physical interpretation but, as we remarked there, it also suffers from a sign problem because it can be negative during unloading. We believe that we have solved this problem in Ref. [1], and shall make extensive use of the technique described there in what follows.

Spaepen [3,4] has introduced an important modification of the above ideas by postulating that the defect density n is directly determined by the excess free volume in the system, v_f, via a relation of the form

$$n \propto \exp\left(-\frac{V^*}{v_f}\right), \qquad (1.3)$$

where V^* is a molecular volume. Spaepen's proposal is that the production term P in Eq. (1.2) should be proportional to the growth rate of v_f. More recently, Johnson et al. [11] have proposed a dynamic free volume model that includes a phenomenological parameter very roughly analogous to the yield stress that emerges from our STZ theory. Unfortunately, Spaepen, Johnson and others (e.g., Ref. [9]) postulate an equation of the form $\dot{v}_f \propto \dot{\epsilon}^{pl}$, which again violates symmetry or analyticity requirements. In short, we believe that these theories require a critical reformulation in order to enable a meaningful atomic-scale analysis of amorphous plasticity.

In addition to reformulating earlier theories of amorphous plasticity, one of our principal goals in this paper is to gain as simple as possible an understanding of recent experimental results on plastic flow in metallic glasses. In particular, we refer to work by Kato et al. [12] on amorphous $Pd_{40}Ni_{10}Cu_{30}P_{20}$, and the results of Lu et al. [13], who measured properties of bulk amorphous $Zr_{41.2}\,Ti_{13.8}\,Cu_{12.5}\,Ni_{10}\,Be_{22.5}$ over a remarkably wide range of strain rates and temperatures.

For the sake of simplicity, we restrict ourselves throughout this paper to the quasilinear theory discussed in Ref. [1]. We also make other assumptions which, as we shall indicate at several places in our presentation, raise fundamental issues regarding nonequilibrium states in deforming solids.

Our order of presentation is as follows. In Sec. II, we review the elements of the low-temperature, quasilinear

theory [1] in a way that prepares concepts and notation for the discussion of thermal relaxation in Sec. III. Section IV is devoted to analysis of these theoretical results and comparison with experiments. Finally, in Sec. V, we return to various fundamental issues that are raised earlier in the paper or are relevant to its conclusions. In particular, we discuss how our original, fully nonlinear STZ theory [10] may need to be invoked in order to make better contact with atomic-scale mechanisms; we briefly address the important issue of shear banding; and we discuss the question of departures from thermodynamic equilibria in driven systems—a question that we shall not be able to avoid in the present analysis.

II. ELEMENTS OF THE LOW-TEMPERATURE STZ THEORY

In order that this account be reasonably self-contained, and to provide some new perspectives about the discussion that follows, we start by reviewing the basic elements of the low-temperature STZ theory.

Throughout the following analysis, we take our original STZ picture [10] more literally than perhaps is necessary. We assume that, instead of being structureless objects as in the earlier theories described in the Introduction, the STZ's are two-state systems. In the presence of a shear stress, they can deform by a finite amount in one direction before becoming jammed and, when jammed in one direction, they can transform in the opposite direction in response to a reversed stress. Importantly, our STZ's are ephemeral; they are created and annihilated during irreversible deformations of the material.

The literal interpretation to be used here requires that all STZ's have approximately the same size and dynamic properties. To visualize such an STZ, think of a void in an elastic material, and place a small group of molecules inside it in such a way that their average free volume is somewhat larger than that for most other molecules in the system. The void has some degree of structural stability; it can deform elastically but, because of the configuration of molecules on its surface, it resists collapse. Rearrangements of the molecules that are caged within the void couple to its shape and therefore to the stress field in the elastic medium in which the void is embedded. This picture suggests that the system undergoes two distinct kinds of irreversible events: volume conserving shear deformations, i.e., the STZ transformations, and dilations or contractions in which the STZ's are created or annihilated. (Nothing in this picture rules out the possibility that transient dilations occur during intermediate stages of the shear transformations.)

For simplicity, as in Refs. [1,10], we consider a two-dimensional model, and we subject this system only to pure shear deformations. As we shall show at the beginning of Sec. IV, the properties of this model are easily reinterpreted in terms appropriate to simple uniaxial stress experiments in three dimensions, so long as we are willing to assume that the system remains spatially uniform. We further restrict ourselves to molecular materials in contact with thermal reservoirs (as opposed to granular materials or foams), so that we may assume that an ambient temperature determines an un-

derlying fluctuation rate. At low temperatures, thermal fluctuations provide an attempt frequency for stress-induced molecular rearrangements, but are too small to activate transitions over energy barriers in the absence of external driving forces. This attempt frequency will never appear explicitly in our analysis but, rather, is embedded in the rate factors to be introduced below.

For present purposes, we need to consider only situations in which the orientation of the principal axes of the stress and strain tensors remains fixed. That is, we do not consider situations in which a fully tensorial version of the STZ theory will be necessary, as in the necking calculations reported in Ref. [14]. Therefore it is sufficient to assume that the population of STZ's consists simply of zones oriented along the two relevant principal axes of the stress tensor. Exactly the same equations as the ones we shall use here can be derived starting from the assumption that the *a priori* distribution of orientations of the zones is continuous and symmetric [15,16]. Without loss of generality therefore we let the deviatoric stress be diagonal along the x, y axes; specifically, let $s_{xx} = -s_{yy} = s$ and $s_{xy} = 0$. Then choose the "+" zones to be oriented (elongated) along the x axis, and the "−" zones along the y axis; and denote the population density of zones oriented in the "+/−" directions by the symbol $n_{\pm}$.

With these conventions, the plastic strain rate is:

$$\dot{\epsilon}_{xx}^{pl} = -\dot{\epsilon}_{yy}^{pl} \equiv \dot{\epsilon}^{pl} = \frac{\lambda}{\tau_0}[R(-s)n_- - R(s)n_+]. \qquad (2.1)$$

Here λ is a material-specific parameter with the dimensions of volume (or area in strictly two-dimensional models), which must be roughly the same order of magnitude as the volume of an STZ, that is, a few cubic or square atomic spacings. The remaining factor on the right-hand side of Eq. (2.1) is the net rate per unit volume at which STZ's transform from "−" to "+" orientations. $R(s)/\tau_0$ and $R(-s)/\tau_0$ are the rates for "+" to "−" and "−" to "+" transitions respectively, where τ_0 is the time scale that characterizes the low-temperature plastic response. For simplicity, we write these rates as explicit functions of only the deviatoric stress s, although they depend implicitly on the temperature and pressure and perhaps other quantities.

The equation of motion for the populations $n_{\pm}$ generally must be a master equation of the form

$$\tau_0 \dot{n}_{\pm} = R(\mp s)n_{\mp} - R(\pm s)n_{\pm} + \Gamma(s, \dots)\left(\frac{n_{\infty}}{2} - n_{\pm}\right).$$

$$(2.2)$$

The first two terms on the right-hand side are the stress-driven transition rates introduced in the preceding paragraph. There is no analog of these terms in Eq. (1.2). They describe volume-conserving, pure-shear deformations which preserve the total population of the STZ's. The last two terms in parentheses, proportional to Γ, describe creation and annihilation of STZ's. In the low-temperature theory, Γ is nonzero only when the plastic strain rate is nonzero; the molecular rearrangements required for creating or annihilating STZ's cannot occur spontaneously, that is, in the absence of external driving forces.

The assumption in Eq. (2.2) that the annihilation and creation rates are both proportional to the same function Γ has serious implications in this theory. Among those implications is the requirement that n_{∞} be a strain-rate independent constant. Note that n_{∞} is the total density of zones generated in a system that is undergoing steady plastic deformation. It is not the same as the quantity n_{eq} introduced in Eq. (1.2), which is the equilibrium density at nonzero temperature and zero strain rate, and ordinarily is said to go rapidly to zero as the temperature decreases below the glass transition. On the other hand, n_{∞} is a property of low-temperature materials at nonzero strain rates.

The form in which we have cast Eq. (2.2) is consistent with a fundamental assumption that we are making about the nature of our low-temperature theory. Specifically, we are assuming that the only relevant time scales at low temperatures are τ_0 and the inverse of the strain rate. This means that, under steady-state conditions at strain rates less than some value of order τ_0^{-1}, the number of events in which the molecules rearrange themselves is not proportional to the time but to the strain. That picture seems intuitively reasonable. If the system requires a certain number of STZ-like rearrangements in order to achieve some deformation, then it should not matter (within limits) how fast that deformation takes place. The picture breaks down, of course, when there are competing rearrangement mechanisms. For example, we shall see that the density of STZ's becomes strain-rate dependent when we introduce thermal fluctuations, because such fluctuations will induce rearrangements at a rate that is independent of the strain rate. We also expect that the picture may fail in polymeric glasses or polycrystalline solids, where more complex components may introduce extra length and time scales.

This simple dimensional argument, leading to a nonzero, rate-independent value of n_{∞}, already hints at a fundamental difficulty in theories of the kind summarized by Eqs. (1.1) and (1.2). These theories have no sensible low-temperature limit because both the strain rate in Eq. (1.1) and the rate factor k_r in Eq. (1.2) vanish rapidly as $T \to 0$. Yet, even at temperatures so low that thermal fluctuations cannot cause molecular rearrangements, such systems must deform irreversibly when sheared.

We shall use the energetic arguments introduced in Ref. [1] to determine the factor Γ in Eq. (2.2), but first we must discuss the state variables and specific forms for the transition rates. We define dimensionless state variables by writing

$$\Lambda \equiv \frac{n_+ + n_-}{n_{\infty}}, \quad \Delta \equiv \frac{n_+ - n_-}{n_{\infty}}. \qquad (2.3)$$

In a more general treatment [14,16,17], Λ remains a scalar density, but Δ becomes a traceless symmetric tensor with the same transformation properties as the deviatoric stress. We also define

$$\mathcal{S} \equiv \frac{1}{2}[R(-s) - R(+s)], \quad \mathcal{C} \equiv \frac{1}{2}[R(-s) + R(+s)], \quad \mathcal{T} \equiv \frac{\mathcal{S}}{\mathcal{C}}. \qquad (2.4)$$

Then the STZ equations of motion become

$$\tau_0\ \dot{\epsilon}^{pl} = \epsilon_0\ \mathcal{C}(s)[\Lambda\ \mathcal{T}(s) - \Delta]; \qquad (2.5)$$

$$\tau_0\dot{\Delta} = 2\ \mathcal{C}(s)[\Lambda\ \mathcal{T}(s) - \Delta] - \Gamma(s,\Lambda,\Delta)\Delta; \qquad (2.6)$$

and

$$\tau_0\dot{\Lambda} = \Gamma(s,\Lambda,\Delta)(1 - \Lambda). \qquad (2.7)$$

Here, $\epsilon_0 \equiv \lambda\ n_\infty$ is roughly the fraction of the total volume of the low-temperature system in steady-state flow that is covered by the STZ's. This is a material-specific quantity. If ϵ_0 is small, then the disorder induced in the system by deformation is small. Conversely, if ϵ_0 is large, then the STZ-like defects cover the system and the material in some sense "melts" under persistent straining.

Throughout this paper, we shall use only what we call the "quasilinear" version of these equations [18]. That is, we note that $\mathcal{T}(s)$ and $\mathcal{C}(s)$ are, respectively, antisymmetric and symmetric dimensionless functions of s, and write

$$\mathcal{T}(s) \cong \frac{s}{s_y} \equiv \tilde{s}; \quad \mathcal{C}(s) \cong 1, \qquad (2.8)$$

where s_y will turn out to be the yield stress. The choice $\mathcal{C}(s) \cong 1$ is, in effect, our definition of the time constant τ_0. As pointed out in earlier papers [1,18], this quasilinear approximation has important shortcomings. Neglecting the stress dependence of $\mathcal{C}(s)$ means that we overestimate the amount of plastic deformation that occurs at small stresses and therefore also overestimate the rate at which orientational memory disappears in unloaded systems. Moreover, the quasilinear approximation is too simplistic to be related directly to atomic mechanisms, a point that we shall comment upon further in Sec. V. Nevertheless, the quasilinear theory has the great advantage that it is mathematically tractable and easy to interpret. It will serve to illustrate the main points that we wish to make in this paper, but aspects of the nonlinearities associated with $\mathcal{C}$ and $\mathcal{T}$ will need to be reintroduced before we shall be able to understand fully the nonequilibrium behavior of amorphous solids.

Equations (2.5)–(2.7) now become

$$\tau_0\dot{\epsilon}^{pl} = \epsilon_0(\Lambda\tilde{s} - \Delta); \qquad (2.9)$$

$$\tau_0\dot{\Delta} = 2(\Lambda\tilde{s} - \Delta) - \Gamma(\tilde{s},\Lambda,\Delta)\Delta; \qquad (2.10)$$

and

$$\tau_0\dot{\Lambda} = \Gamma(\tilde{s},\Lambda,\Delta)(1 - \Lambda). \qquad (2.11)$$

The quantity $n_\infty\ \Gamma/\tau_0$ is the STZ creation rate and therefore plays exactly the same role as the phenomenological defect production rates that we discussed—and complained about—in the Introduction. We can derive an expression for that rate by using the energy-balance argument introduced in Ref. [1]. As before, we start by writing the first law of thermodynamics in the form

$$2\dot{\epsilon}^{pl}s = \frac{2\epsilon_0 s_y}{\tau_0}(\Lambda\tilde{s} - \Delta)\tilde{s} = \epsilon_0 s_y\frac{d}{dt}\psi(\Lambda,\Delta) + \mathcal{Q}(\tilde{s},\Lambda,\Delta). \qquad (2.12)$$

The left-hand side of Eq. (2.12) is the rate at which plastic work is done by the applied stress $s = s_y\tilde{s}$. On the right-hand side, $\epsilon_0\ s_y\ \psi$ is the state-dependent recoverable internal energy, and $\mathcal{Q}$ is the dissipation rate. So long as the STZ's remain uncoupled from the heat bath, $\mathcal{Q}$ must be positive in order for the system to satisfy the second law of thermodynamics, that is, for the work done in going around a closed cycle in the space of variables s, Λ, and Δ to be nonnegative.

As argued in Ref. [1], the simplest and most natural choice for Γ—and, so far as we can tell, the only one that produces a sensible theory—is that it be the energy dissipation rate per STZ. That is,

$$\mathcal{Q}(\tilde{s},\Lambda,\Delta) = \frac{\epsilon_0 s_y}{\tau_0}\Lambda\Gamma(\tilde{s},\Lambda,\Delta). \qquad (2.13)$$

With this hypothesis, we can use Eqs. (2.10) and (2.11) to write Eq. (2.12) in the form

$$2(\Lambda\tilde{s} - \Delta)\tilde{s} = \frac{\partial\psi}{\partial\Lambda}\Gamma(1 - \Lambda) + \frac{\partial\psi}{\partial\Delta}[2(\Lambda\tilde{s} - \Delta) - \Gamma\Delta] + \Lambda\Gamma. \qquad (2.14)$$

Then, solving for Γ, we find

$$\Gamma = \frac{2(\Lambda\tilde{s} - \Delta)(\tilde{s} - \partial\psi/\partial\Delta)}{\Lambda + (1 - \Lambda)(\partial\psi/\partial\Lambda) - \Delta(\partial\psi/\partial\Delta)}. \qquad (2.15)$$

To assure that Γ remains non-negative for all $\tilde{s}$, we must let

$$\frac{\partial\psi}{\partial\Delta} = \frac{\Delta}{\Lambda}, \qquad (2.16)$$

so that the numerator becomes $2\ \Lambda\ (\tilde{s} - \Delta/\Lambda)^2$. Then (see Ref. [1]), we choose

$$\psi(\Lambda,\Delta) = \frac{\Lambda}{2}\left(1 + \frac{\Delta^2}{\Lambda^2}\right), \qquad (2.17)$$

so that

$$\Gamma(\tilde{s},\Lambda,\Delta) = \frac{4\Lambda(\Lambda\tilde{s} - \Delta)^2}{(1 + \Lambda)(\Lambda^2 - \Delta^2)}. \qquad (2.18)$$

This result has the physically appealing feature that it diverges when Δ^2 approaches its upper limit Λ^2, thus enforcing a natural boundary for dynamical trajectories in the space of the state variables Λ and Δ.

It is convenient at this point to replace the variable Δ by $m = \Delta/\Lambda$, so that the equations of motion become

$$\tau_0\dot{\epsilon}^{pl} = \epsilon_0\Lambda(\tilde{s} - m); \qquad (2.19)$$

$$\tau_0\dot{m} = 2(\tilde{s} - m)\left[1 - \frac{2m(\tilde{s} - m)}{(1 + \Lambda)(1 - m^2)}\right]; \qquad (2.20)$$

and

$$\tau_0 \frac{\dot{\Lambda}}{\Lambda} = \left[\frac{4(\tilde{s} - m)^2}{1 - m^2} \right] \left(\frac{1 - \Lambda}{1 + \Lambda} \right). \qquad (2.21)$$

At the stable fixed point of Eq. (2.21), $\Lambda = 1$, Eq. (2.20) becomes

$$\tau_0 \dot{m} = \frac{2(\tilde{s} - m)(1 - \tilde{s}m)}{(1 - m^2)}, \qquad (2.22)$$

which exhibits explicitly the exchange of stability at $\tilde{s} = 1$ between jammed states with $m = \tilde{s}$ and flowing states with $m = 1/\tilde{s}$.

III. THERMAL EFFECTS

We return now to Eq. (2.2), the low-temperature master equation for the STZ population densities $n_\pm$, and ask what changes need to be made in order to incorporate thermal effects at temperatures near the glass transition. One obvious possibility is to modify the rate factors $R(\pm s)$ to include thermal activation across energy barriers; indeed, we eventually shall have to do that (see Sec. V). However, our quasilinear approximation makes it difficult to do this systematically.

The more important thermal effects are those that are completely missing in Eq. (2.2), specifically, the thermally assisted relaxation—i.e., aging—of the STZ variables that can occur spontaneously in the absence of external driving or plastic strain rate. There are two ways in which relaxation must occur. First, thermal fluctuations ought to act much like deformation-induced disorder in causing the $n_\pm$ to relax toward their steady-state values $n_\infty/2$. Second, there should be some annealing mechanism that causes the total STZ population to decrease. Both of these mechanisms involve dilations and contractions of the kind associated with creation and annihilation of STZ's; thus, again for simplicity, we assume that there is just a single relaxation rate, denoted $\rho(T)/\tau_0$, that characterizes them. As we shall see, that rate will have the Vogel-Fulcher or Cohen-Grest [19] form, rapidly becoming extremely small as the temperature T falls below the glass temperature. Specifically we expect that $\rho(T)$ has the form

$$\rho(T) = \rho_0 \exp\left(-\frac{\Delta V^{dil}}{v_f(T)} \right), \qquad (3.1)$$

where ρ_0 is a dimensionless prefactor, ΔV^{dil} is the activation volume required to nucleate a dilational rearrangement, and $v_f(T)$ is usually identified as the free volume. The Cohen-Grest approximation for $v_f(T)$ has the form

$$\frac{v_f(T)}{v_0} = T - T_0 + \sqrt{(T - T_0)^2 + T_1 T}, \qquad (3.2)$$

where v_0, T_0 and T_1 are fitting parameters. This expression was found by Masuhr *et al.* [20] and Lu *et al.* [13] to provide a fairly accurate fit to their data. (We shall not use this formula explicitly in what follows.)

In accord with the preceding remarks, our proposed form for the modified master equation is

$$\tau_0 \dot{n}_\pm = R(\mp s)n_\mp - R(\pm s)n_\pm + [\Gamma(s,\Lambda,\Delta) + \rho(T)]\left(\frac{n_\infty}{2} - n_\pm \right)$$

$$- \kappa \, \rho(T)\left(\frac{n_+ + n_-}{n_\infty} \right)n_\pm. \qquad (3.3)$$

The first and second appearances of $\rho(T)$ on the right-hand side of Eq. (3.3) correspond, respectively, to its two roles described above. The second of these terms, the quadratic form with a dimensionless multiplicative constant κ, is similar to the n^2 term on the right-hand side of Eq. (1.2). This bimolecular mechanism has been discussed extensively in Refs. [21–23].

Equations (2.9)–(2.11) now become

$$\tau_0 \dot{\epsilon}^{pl} = \epsilon_0(\Lambda \tilde{s} - \Delta) \qquad (3.4)$$

(unchanged from before);

$$\tau_0 \dot{\Delta} = 2(\Lambda \tilde{s} - \Delta) - [(\Gamma \tilde{s}, \Lambda, \Delta) + \rho(T)]\Delta - \kappa \rho(T)\Lambda\Delta; \qquad (3.5)$$

and

$$\tau_0 \dot{\Lambda} = [\Gamma(\tilde{s}, \Lambda, \Delta) + \rho(T)](1 - \Lambda) - \kappa \, \rho(T)\Lambda^2. \qquad (3.6)$$

The next step is to repeat the energy-balance analysis of Eqs. (2.12)–(2.18) to recompute the function $\Gamma(\tilde{s}, \Lambda, \Delta)$. We assert that Eq. (2.13) relating Γ and the dissipation rate $\mathcal{Q}$ must remain unchanged by the addition of the thermal relaxation terms in Eq. (3.3). That is, Γ in Eq. (3.3) must be the energy dissipated per STZ when plastic work is done on the system. The expression for the internal energy $\psi(\Lambda, \Delta)$ must remain as given by Eq. (2.17) because Eq. (2.16) is still required by the non-negativity condition. The result, after inserting the terms proportional to $\rho(T)$ into Eqs. (2.14) and (2.15), and transforming to $m = \Delta/\Lambda$, is

$$\Gamma(\tilde{s}, \Lambda, m) + \rho(T)$$

$$= \Lambda \left[\frac{4 \, (\tilde{s} - m)^2 + 2 \, \rho(T) + \kappa \, \rho(T)\Lambda(1 + m^2)}{(1 + \Lambda)(1 - m^2)} \right]$$

$$\equiv \Lambda \tilde{\Gamma}(\tilde{s}, \Lambda, m, T). \qquad (3.7)$$

Note that $\tilde{\Gamma}$ is non-negative, as is necessary because it is a prefactor for the annihilation and creation rates. The non-negativity condition no longer strictly applies to Γ itself because the system is now coupled to the heat bath.

The new equations of motion for m and Λ are

$$\tau_0 \, \dot{\epsilon}^{pl} = \epsilon_0 \, \Lambda(\tilde{s} - m), \qquad (3.8)$$

$$\tau_0 \dot{m} = 2(\tilde{s} - m) - m\tilde{\Gamma}(\tilde{s}, \Lambda, m, T), \qquad (3.9)$$

and

$$\tau_0 \frac{\dot{\Lambda}}{\Lambda} = \tilde{\Gamma}(\tilde{s}, \Lambda, m, T)(1 - \Lambda) - \kappa \, \rho(T)\Lambda. \qquad (3.10)$$

As in previous presentations, we recover Bingham-like plasticity for small ρ and for stresses above s_y, i.e., $\tilde{s} > 1$. In that case, the equations of motion revert to Eqs.

(2.19)–(2.21) so that, in steady state, $\Lambda \rightarrow 1$ and $m \rightarrow 1/\tilde{s}$. Thus

$$\dot{\epsilon}^{pl} \approx \frac{\epsilon_0}{\tau_0}\left(\tilde{s} - \frac{1}{\tilde{s}}\right); \quad \tilde{s} > 1. \tag{3.11}$$

This theory exhibits no power-law rheology for flow above the yield stress. As we shall see, however, it does exhibit behavior that looks like superplasticity.

The more interesting behavior is thermally assisted creep below the yield stress, $\tilde{s} < 1$, and the transition between creep and flow near $\tilde{s} = 1$. For present purposes, we only need to consider cases in which $\rho(T) \ll 1$. In the steady-state creep region where $\tilde{s} \ll 1$ and $m \cong \tilde{s}$, Eqs. (3.7) and (3.9) tell us that $\tilde{s} - m$ is small of order $m\rho$. Then the quantity $(\tilde{s} - m)^2$ in the numerator of $\tilde{\Gamma}$ is negligible compared to the other terms. The steady-state version of Eq. (3.10) becomes simply

$$1 - \Lambda_N(\kappa) \approx \kappa \, \Lambda_N^2(\kappa); \quad \Lambda_N(\kappa) = \frac{1}{2\,\kappa}(\sqrt{1 + 4\,\kappa} - 1),$$
$$\tag{3.12}$$

where the subscript N denotes the low-stress Newtonian limit.

In the complete absence of a driving stress $\tilde{s}$, the exact steady-state solutions of Eqs. (3.9) and (3.10) are $m = 0$ and $\Lambda = \Lambda_N(\kappa)$. Thus the analog of n_{eq} in Eq. (1.2) is $n_\infty \Lambda_N(\kappa)$, which is a temperature-independent quantity instead of being, as is usually assumed, a rapidly varying function of the form $\exp[-\Delta V^{dil}/v_f(T)]$. Indeed, the temperature dependence of n_{eq} is often invoked in the context of equations such as Eq. (1.2) to interpret calorimetric data [9,24]. Because of its lack of a temperature-dependent n_∞, our present theory cannot predict the specific heat peak near the glass transition that is seen by the latter authors. We could fix this problem in an *ad hoc* manner by assigning some temperature dependence to n_∞ and/or κ. However, such a procedure would simply gloss over the fundamental difficulty that we are facing here—that the limiting steady-state value of Λ must depend upon the order in which we take the limits $T \rightarrow 0$ and $\dot{\epsilon}^{pl} \rightarrow 0$, but that no such behavior appears in our equations. This is the same situation that we discussed in the paragraphs following our first introduction of n_∞ in Eq. (2.2); we shall return to it in Sec. V. For the present, we leave the situation as is, with a temperature-independent Λ_N, and with the understanding that we cannot yet use these equations to describe behavior much above the glass temperature.

To compute the viscosity, it is easiest first to set $\dot{m} = \dot{\Lambda} = 0$ in Eqs. (3.9) and (3.10) and eliminate $\tilde{\Gamma}$ to find

$$(\tilde{s} - m)(1 - \Lambda) = \frac{\kappa \rho(T)}{2} m \Lambda, \tag{3.13}$$

which is an exact relationship between the steady-state values of $\tilde{s}$, Λ and m at any strain rate. Combining these results in the limit $\tilde{s} \approx m \rightarrow 0$, we compute the Newtonian viscosity η_N:

$$\eta_N \equiv \lim_{\dot{\epsilon}^{pl} \rightarrow 0} \frac{s}{2 \, \dot{\epsilon}^{pl}} = \frac{s_y \tau_0}{\epsilon_0 \rho(T)}, \tag{3.14}$$

which confirms our expectation that $\rho(T)$ is the rate function that governs viscous relaxation.

IV. ANALYSIS AND COMPARISON WITH EXPERIMENTS

Before making comparisons with experiments, we must return to the question of how to generalize our two-dimensional theory into one that can be applied to three-dimensional experiments. The basic structure of our equations of motion must be preserved, with due respect for the relevant symmetries, in any generalization of this theory to higher dimensions. That is, our variables $\tilde{s}$, $\dot{\epsilon}^{pl}$, and m must become traceless symmetric tensors, and Λ must remain a scalar, so that Eqs. (3.8) and (3.9) become

$$\tau_0 \, \dot{\epsilon}_{ij}^{pl} = \epsilon_0 \, \Lambda(\tilde{s}_{ij} - m_{ij}), \tag{4.1}$$

and

$$\tau_0 \, \dot{m}_{ij} = 2(\tilde{s}_{ij} - m_{ij}) - \tilde{\Gamma}(\tilde{s}, \Lambda, m, T) m_{ij}. \tag{4.2}$$

The energy-balance analysis yields

$$\tilde{\Gamma}(\tilde{s}, \Lambda, m, T)$$
$$= \frac{2(\tilde{s}_{ij} - m_{ij})(\tilde{s}_{ij} - m_{ij}) + 2\rho(T) + \kappa\rho(T)\Lambda(1 + \bar{m}^2)}{(1 + \Lambda)(1 - \bar{m}^2)}, \tag{4.3}$$

where we are using the summation convention, and $\bar{m}^2 = (1/2) m_{ij} m_{ij}$.

The experiments in which we are interested involve only uniaxial stresses, say, in the x direction. If there are no tractions in the y or z directions, and if we can ignore spatial nonuniformities, then the total stress σ_{ij} is diagonal with $\sigma_{xx} = \sigma$, $\sigma_{yy} = \sigma_{zz} = 0$. Similarly, for the deviatoric stress, $\tilde{s}_{yy} = \tilde{s}_{zz} = -\tilde{s}_{xx}/2$; and $m_{yy} = m_{zz} = -m_{xx}/2$. Thus $\bar{m}^2 = 3/4 \, m_{xx}^2$. We can now make the xx components of Eqs. (4.1) and (4.3) look exactly like Eqs. (3.8), (3.9), and (3.7) by defining $m^2 = \bar{m}^2$, $m = \sqrt{3/4} \, m_{xx}$, $\tilde{s} = \sqrt{3/4} \, \tilde{s}_{xx}$, $\dot{\epsilon}^{pl} = \dot{\epsilon}_{xx}^{pl}$, and by replacing ϵ_0 by $\epsilon_0' = \sqrt{4/3} \, \epsilon_0$. Note that the dynamical exchange of stability, i.e., plastic yielding, still occurs at $\tilde{s} = 1$; thus our scaling of the stress by s_y remains correct. When comparing to the data, which is presented in terms of the uniaxial stress $\sigma = \sigma_{xx}$, we write $\sigma = (3/2)s_{xx} = \sqrt{3}s_y\tilde{s}$ or, equivalently, $\sigma = \sigma_y\tilde{s}$, where σ_y is the tensile yield stress. Equation (3.14), however, remains unchanged with ϵ_0 rather than ϵ_0', because viscosity now is expressed as $\eta = s_{xx}/2\dot{\epsilon}_{xx}^{pl} = s/\sqrt{3}\dot{\epsilon}^{pl}$.

To illustrate the principal results of our analysis, we first follow the lead of Kato *et al.* [12] and Lu *et al.* [13] by looking for scaling in the steady-state behavior of our system. To be specific about what we mean here, we show in Figs. 1 and 2 sets of stress-strain curves for various temperatures and fixed strain rates. As we shall explain shortly, these figures are to be compared with Figs. 1 and 2 in Ref. [13]. (See also Fig. 1 in Ref. [9] and Fig. 1 in Ref. [12].) A general feature of these curves is that, when the strain rate is held
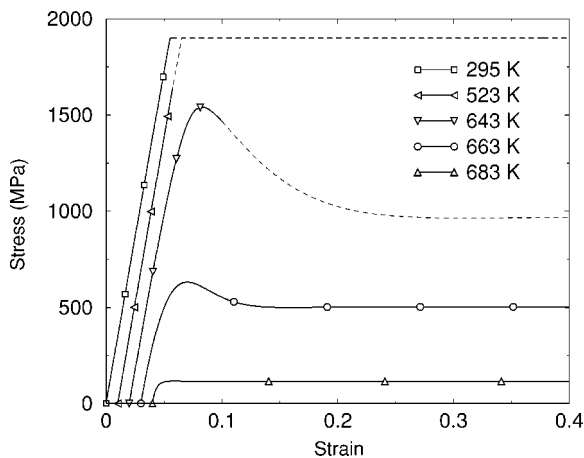
FIG. 1. Theoretical curves of tensile stress versus strain for the bulk metallic glass $Zr_{41.2}Ti_{13.8}Cu_{12.5}Ni_{10}Be_{22.5}$ at several different temperatures as shown. The strain rate is $\dot{\epsilon}^{total}=1\times10^{-1}$ s^{-1}. For clarity, the curves have been displaced by constant increments along the strain axis.

FIG. 3. Scaling behavior in the STZ theory: shear stress $\tilde{s}$ as a function of strain rate scaled by η_N. This graph is plotted for the same set of temperatures as shown in Fig. 4(a), but for a larger range of strain rates.

constant, the stress rises through a maximum, decreases as the material softens, and then reaches a steady-state value. We shall discuss the initial transients later in this section, but look first at the late-stage, steady-state behavior.

We compute the steady-state flow stress as a function of the strain rate by solving Eqs. (3.9) and (3.10) with $\dot{m}=\dot{\Lambda}=0$. Then, as in Ref. [12,13], we plot $\tilde{s}=s/s_y$ as a function of $\eta_N\dot{\epsilon}^{pl}$ for eight different values of the relaxation rate $\rho(T)$ corresponding to the eight different temperatures for which data are reported in Ref. [13]. The results are shown in Fig. 3. As discovered by Kato *et al.* [12], all of these curves lie on top of one another for stresses $\tilde{s}<1$ but, in our case, they diverge from each other in the flowing regime, $\tilde{s}>1$, where the Bingham-like behavior shown in Eq. (3.11) sets in.

Figure 4(a) contains the same theoretical curves as those shown in Fig. 3, but plotted there as tensile stress versus
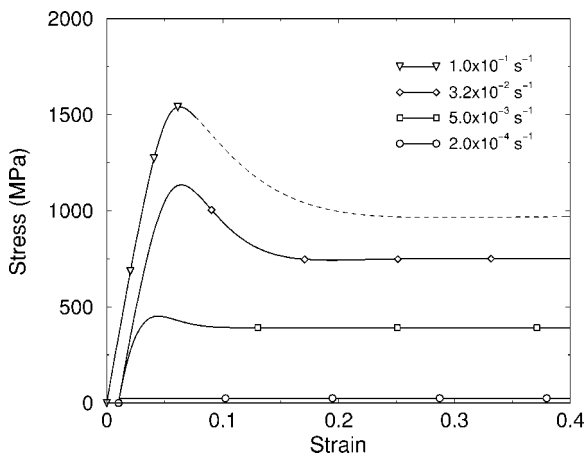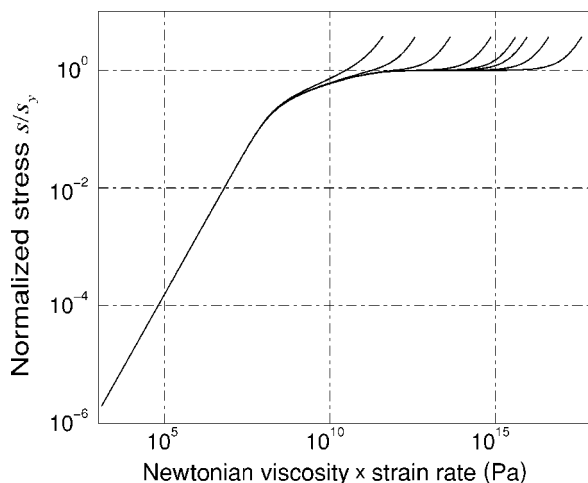
scaled strain rate, and compared with experimental data taken from Fig. 9(a) of Ref. [13]. The same theoretical functions and data points are replotted in Fig. 4(b) to show the normalized viscosity, η/η_N as a function of the scaled strain rate. The latter figure is directly comparable to Ref. [13], Fig. 9(b). Note that the range of strain rates shown in Figs. 4 corresponds to the range of the experimental data and is substantially smaller than that shown in Fig. 3. The theoretical curve that lies above the rest at high strain rates is for T
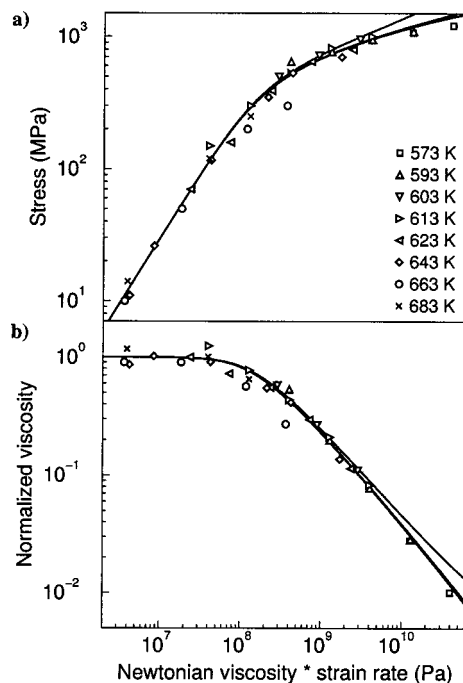

FIG. 4. Tensile stress and viscosity as functions of scaled strain rate $\eta_N\dot{\epsilon}^{total}$. The data points for the bulk metallic glass $Zr_{41.2}Ti_{13.8}Cu_{12.5}Ni_{10}Be_{22.5}$ are taken from Ref. [13], Figs. 9(a) and 9(b). The solid curves are theoretical results computed for the same set of temperatures as shown.

FIG. 2. Theoretical curves of tensile stress versus strain for the bulk metallic glass $Zr_{41.2}Ti_{13.8}Cu_{12.5}Ni_{10}Be_{22.5}$ at several different strain rates as shown. The temperature is $T=643$ K. For clarity, all but the first of these curves have been displaced by the same amount along the strain axis.
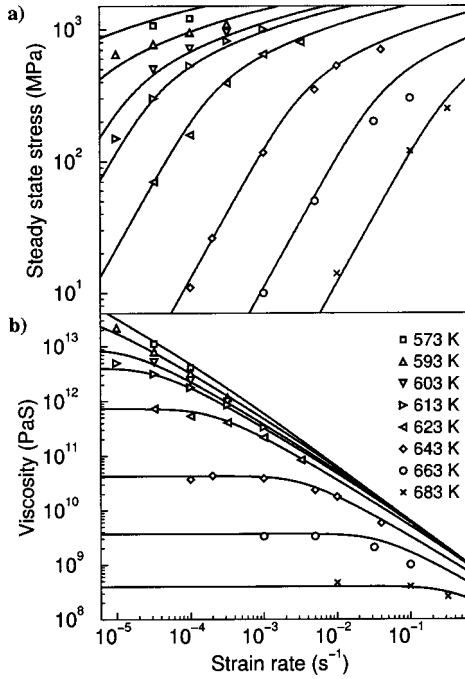
FIG. 5. Tensile stress (a) and viscosity (b) as functions of strain rate for different temperatures as shown. The data points are for the bulk metallic glass $Zr_{41.2}Ti_{13.8}Cu_{12.5}Ni_{10}Be_{22.5}$ as reported by Ref. [13], Figs. 7 and 8. The solid lines are theoretical curves.

=683 K, the highest of the temperatures reported in Ref. [13]. The data points at that temperature all lie at scaled strain rates that are too small to test this predicted breakdown of the scaling law.

Our Fig. 5(a) shows individual theoretical and experimental curves of tensile stress as a function of (unscaled) strain rate for different temperatures. Here, the experimental data are from Ref. [13], Fig. 7. These curves are replotted in Fig. 5(b) to show (unscaled) viscosity as a function of strain rate, analogous to Ref. [13], Fig. 8.

In constructing these figures, we have determined our theoretical parameters as follows:

We have used the value of the room-temperature tensile yield stress reported in Ref. [13], $\sigma_y = 1.9$ GPa. Thus $\sigma = 1.9\tilde{s}$ GPa.

Rather than using the Cohen-Grest formula with parameters from Ref. [20], we have taken the limiting (vanishing strain rate) Newtonian viscosities directly from Ref. [13], Fig. 10, and have checked that these values (apart from one apparently misplaced point) are consistent with the data points in Ref. [13], Fig. 9.

Given the above constraints, we are left with only two parameters, κ and ϵ_0/τ_0 (or, equivalently, ϵ_0'), that can be adjusted to fit the steady-state experimental data in Ref. [13], Fig. 7. Because we know experimental values for the limit-

ing viscosities $\eta_N(T)$ at different temperatures, a value for the ratio ϵ_0/τ_0 in Eq. (3.14) determines the overall scale factor for the function $\rho(T)$. Thus our fitting procedure has been to start by choosing values of κ and ϵ_0/τ_0. We then use those values to determine $\rho(T)$ and to compute steady-state solutions of Eqs. (3.9), (3.10), and (2.19). From these solutions we compute steady-state stress versus strain-rate relations that can be compared with the experimental data. We then iterate this process to find best-fit values for κ and ϵ_0/τ_0.

Our best-fit parameter values, obtained by the procedure outlined above, are $\kappa = 120$ and $\epsilon_0/\tau_0 = 260$ s^{-1}. Our corresponding values of $\rho(T)$, along with our estimates of the viscosities, are shown in Table I. We emphasize that these values are not much better than order-of-magnitude estimates.

As is obvious in Fig. 5, there is scatter in the experimental data, and there may also be systematic errors. For example, the two points at the highest strain rates for $T = 663$ K fall well below our theoretical curve for that temperature while the theoretical fits look good for the temperatures on either side, i.e., $T = 643$ and 683 K. We could improve the fits to all three of these curves by choosing a substantially larger value of κ; but we would do this at the expense of poorer fits at lower temperatures. However, the values of the viscosities that we can deduce from Ref. [13], Fig. 10 seem uncertain, possibly by factors of 2 or 3; so our estimates of $\rho(T)$ and therefore all our theoretical curves—especially those at the lower temperatures—might be modified by more accurate viscosity data.

Within the above uncertainties, our theoretical fits to the experimental data are relatively insensitive to our choices of the two parameters that we have allowed ourselves. On the one hand, this insensitivity gives us confidence in the basic structure of our theory; on the other hand, it means that we cannot yet test the theory in as much detail as we would like. For example, the yield stress s_y probably ought to be a function of temperature, decreasing slowly (in contrast to the rapidly varying viscosity) from room temperature through the experimental range. Its behavior should be roughly like that of the shear modulus, which must soften as the system approaches the glass transition. Also, as we have discussed above, we expect that ϵ_0 ultimately will be temperature dependent because it is proportional to n_∞. We could improve the fits, for example, at the lower temperatures shown in Fig. 5, by incorporating such temperature dependences into our equations; but it seems to make little sense to do so without first resolving various uncertainties in both the theory and the experiments.

Our main conclusion from this steady-state analysis is that we are observing a transition from thermally assisted creep to viscoplastic flow in the neighborhood of the dynamic yield stress. At low stresses and strain rates, the linear response

TABLE I. Experimental data for viscosity taken from Ref. [13], and values of ρ used in the present calculations.

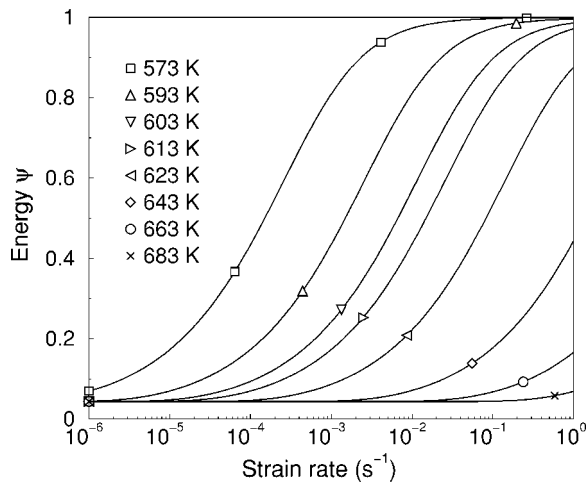| Temperature K	573	593	603	613	623	643	663	683
Viscosity (PaS)	4.00×10^{14}	4.03×10^{13}	8.99×10^{12}	4.03×10^{12}	7.29×10^{11}	4.27×10^{10}	3.68×10^9	3.99×10^8
ρ	1.07×10^{-8}	1.06×10^{-7}	4.77×10^{-7}	1.06×10^{-6}	5.88×10^{-6}	1.01×10^{-4}	1.17×10^{-3}	1.15×10^{-2}

FIG. 6. Dimensionless energy ψ as a function of strain rate for the same set of temperatures shown in the preceding figures.

relation contains only the factor $\eta_N \propto 1/\rho(T)$, thus we obtain the simple scaling. Near the yield stress, however, our theoretical strain rate increases by several orders of magnitude for small increments of stress, and the experimental behavior tracks this trend accurately. This behavior resembles superplasticity. Interestingly, the theoretical scaling persists through the "superplastic" region and does not break down until true viscoplastic flow begins.

Before returning to the transient stress-strain curves shown in Figs. 1 and 2, we show one other steady-state prediction of our theory for which there are no data in Ref. [13], but which seems to be potentially important. In Fig. 6, we have used our steady-state solutions for m and Λ to plot the dimensionless internal energy $\psi = (\Lambda/2)(1+m^2)$ as a function of the strain rate $\dot{\epsilon}^{pl}$, for the set of temperatures used in the preceding figures. The energy ψ might be measured by differential scanning calorimetry (DSC), as has been done by Hasan and Boyce in studies of polymeric glasses [25,26]. De Hey *et al.* [9] also report DSC results, which they interpret as measurements of free volume. We assume that Fig. 4 in Ref. [9], apart from the scale on the vertical axis, is at least qualitatively the same as a graph of ψ versus strain rate analogous to our Fig. 6. The two figures are similar to one another if we look at our theoretical curves only at small strain rates.

An important feature of our Fig. 6 is that, at fixed strain rate, ψ decreases as T increases. That trend is exactly what we expect for thermally assisted creep; the higher the temperature, the fewer STZ's are needed in order to sustain a given flow rate, and thus the smaller the internal energy. Note, however, that our theory predicts that all of these curves converge to a single, temperature independent, value $\psi \to \Lambda_N(\kappa)/2$ in the limit $\dot{\epsilon}^{pl} \to 0$. On the other hand, De Hey *et al.* plausibly assert that the equilibrium value of the STZ density, n_{eq}, should be an increasing function of temperature. If so, these curves must cross each other and the trend in temperature dependence must be reversed at small enough values of $\dot{\epsilon}^{pl}$. An extension of these measurements to smaller strain rates might therefore provide a test of our differing assumptions about the STZ density n_{eq}.

So far, we have examined only steady-state behavior. We turn next to stress-strain curves obtained in constant strain-

rate experiments such as those shown in our Figs. 1 and 2 and in Figs. 1 and 2 of Ref. [13]. To plot these curves, we solve

$$\frac{\sigma_y}{E}\dot{\tilde{s}} = \dot{\epsilon}_{xx}^{total} - \sqrt{\frac{4}{3}}\frac{\epsilon_0}{\tau_0}\Lambda(\tilde{s}-m), \qquad (4.4)$$

along with Eqs. (3.9) and (3.10) to compute $\tilde{s}$ as a function of the total strain. We use the value of Young's modulus given in Ref. [13], $E=96$ GPa, to estimate $E/\sigma_y \cong 50$. For time-dependent calculations, we must choose a value of the time scale τ_0, which multiplies the time derivatives in Eqs. (3.9) and (3.10). To do this, we keep the ratio ϵ_0/τ_0 fixed at its value obtained from the steady-state calculations, and we adjust the value of ϵ_0 so as to fit the transient stress-strain curves. Our best-fit value is $\epsilon_0=0.7$, which means that $\tau_0 \cong 2.7 \times 10^{-3}$ s. We emphasize that this value, like our estimates for κ and ϵ_0/τ_0, remains highly uncertain. It is possible that we may eventually be able to sharpen our estimate of the time scale τ_0 by using the time-dependent stress-relaxation data shown in Ref. [13]. In fact, we can reproduce those results about as well as the other results shown here, but our theory in this case is especially sensitive to our quasilinear approximation plus other uncertainties regarding the experiments.

Our Figs. 1 and 2 are drawn so as to be directly comparable to Figs. 1 and 2 in Ref. [13]; that is, we use the same strain rates and temperatures. The one other parameter that we must choose for solving Eqs. (3.9), (3.10), and (4.4) is the initial value of Λ, which we denote by Λ_0. Theoretically, the smallest value of Λ_0 that can be achieved by annealing is $\Lambda_N(\kappa)=0.087$ (for $\kappa=120$); therefore we have used this value of Λ_0 for these two figures. The initial values of m and $\tilde{s}$ are always chosen to be zero.

In all cases, the agreement between theory and experiments seems satisfactory given the various uncertainties. The peak heights and positions for fixed strain rate $\dot{\epsilon}^{total} = 0.1$ s^{-1} and varying temperatures in Fig. 1, and for fixed temperature $T=643$ K and varying strain rates in Fig. 2, are within about ten percent of their experimental values. The experimental curves for low temperatures and large strain rates end where the samples break; the dashed lines in our figures indicate our theoretical extensions of those parts of the curves for which no experimental data is available. The one systematic discrepancy is that our initial theoretical slopes are smaller than the experimental ones. This is an artifact of our quasilinear approximation, which ignores the strong stress and temperature dependence of the factor $C(s)$ in Eqs. (2.5) and (2.6) (see remarks in Sec. V). In the limit of low temperatures and very small strain rates, our theory predicts this initial slope to be $E/(1+E\,\epsilon_0'\,\Lambda_0/2\sigma_y)$ instead of simply E. This does not happen in the fully nonlinear theory presented in Ref. [10]. We have chosen not to include these nonlinear effects in our calculations here because they introduce additional undetermined parameters, and they are not necessary to describe the shear softening and shear thinning observed at higher stresses near the glass transition temperature.
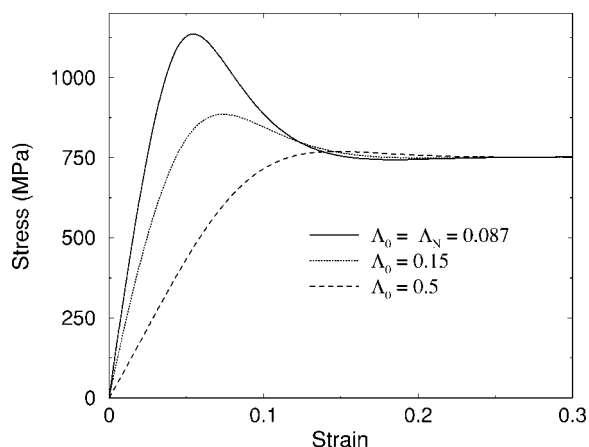
FIG. 7. Tensile stress as a function of strain for several different values of Λ_0. Curves are plotted for $\dot{\epsilon}^{total} = 3.2 \times 10^{-2}$ s^{-1} at $T = 643$ K.

Finally, in Fig. 7, we use the material parameters deduced above for the system studied in Ref. [13] to plot stress-strain curves for different Λ_0's, all at temperature $T=643$ K and $\dot{\epsilon}^{total} = 3.2 \times 10^{-2}$ s^{-1}. The different Λ_0's correspond to different initial states of disorder produced by varying the annealing times and temperatures. Presumably, annealing for longer times at lower temperatures produces smaller values of Λ_0; but it seems difficult to make quantitative estimates of this effect. These curves may be compared qualitatively with those shown in Ref. [9], Fig. 9, where larger initial densities of STZ's produce larger plastic responses and correspondingly smaller overshoots during the early stages of deformation.

V. CONCLUDING REMARKS

The comparison with experiments discussed in the preceding section leads us to believe that the STZ theory captures the main features of the experimental data, but that we shall have to improve it in specific respects if we are to develop it into a yet more quantitative, predictive description of plastic deformation in amorphous solids. We conclude this paper by identifying three directions for the next phases of these investigations.

Fully nonlinear, temperature-dependent transition rates: When we examine the quasilinear STZ theory in the context of a theory that includes thermal fluctuations, we see that it is a special case in which the shear rearrangements are not being modeled as realistically as the dilations or contractions. To see this in more detail, go back to our original Ref. [10], fully nonlinear version of the low-temperature rate factors $R(s)$:

$$R(s) = \frac{1}{\tau_0}\exp\left(-\frac{\Delta V^{shear}(s)}{v_f}\right); \quad \Delta V^{shear}(s) = \Delta V_0^{shear}\, e^{-s/\bar{\mu}},$$

(5.1)

where $\Delta V^{shear}(s)$ is the activation volume required to nucleate a shear transformation. Our idea here was that, at tem-

peratures well below the glass temperature, the transitions between STZ states are not thermally activated but, rather, are controlled entropically. That is, the rate factors are determined by the number of paths that the molecules within a zone can follow in moving around each other while going from one state to the other. The exponential factor in Eq. (5.1) is an approximation for a weighted measure of that number of paths. Its s dependence means that greater weight must be given to paths moving in the direction of the stress than opposite to it. The exponential form of $\Delta V^{shear}(s)$ is the simplest non-negative function that becomes arbitrarily small at large s and introduces just one new parameter, the effective STZ stiffness $\bar{\mu}$. The quasilinear version of the theory corresponds (roughly) to the limit of small s and small values of $\Delta V_0^{shear}/v_f$.

Comparison of Eq. (5.1) with Eq. (3.1) indicates that the natural way to include thermal effects in $R(s)$ is simply to let v_f have the T-dependent Cohen-Grest form shown in Eq. (3.2). This means that, at low T, the ratio $\Delta V_0^{shear}/v_f(T)$ becomes very large, which, in turn, implies that the functions $\mathcal{C}(s)$ and $\mathcal{T}(s)$ introduced in Eq. (2.4) become strongly stress dependent, and the quasilinear approximations made in Eqs. (2.8) are no longer valid. Importantly, $\mathcal{C}(s)$ becomes very small for small s, so that plastic deformation is strongly suppressed at stresses appreciably below the yield stress.

The strong stress dependence of $\mathcal{C}(s)$ and $\mathcal{T}(s)$ should be especially apparent in transient behavior of the kind shown in Figs. 1, 2, and 7. Here, the initial response to loading at small stress will be almost entirely elastic, and plastic deformation will begin only later in the process. We shall have to use the fully nonlinear theory when undertaking more detailed comparisons with these kinds of experimental results.

Shear localization: All of the analysis in this paper pertains to spatially homogeneous systems. In order to make closer contact with experiments, we shall have to understand why and when these systems become unstable against shear banding and inhomogeneous failure modes, especially fracture.

One mechanism for shear localization that we have not mentioned in this presentation is the elastic interaction between STZ's studied in Ref. [17]. As shown in that paper, an STZ-like event generates a quadrupolar stress field that induces other nearby events along preferred spatial directions and suppresses events elsewhere. The result is a tendency toward shear localization that should be interesting to examine in the context of this more general version of the STZ theory.

A second mechanism that seems likely to play a role in shear localization is already built into our equations of motion when we write them in terms of spatially varying fields. From Eqs. (3.7) and (3.10), we see that the STZ density Λ grows most rapidly, within limits, in regions where Λ already is large. This feedback effect, perhaps coupled to the effect of elastic interactions mentioned above, is our best guess at present about how shear banding will emerge in the STZ theory.

Effective temperature and the interpretation of n_{eq}: Finally, we return to Spaepen's suggestion that the density of STZ's might be directly related to the free volume as in Eq.

(1.3). Note that v_f appears in that equation, not as an extensive quantity related directly to the difference between the actual volume and some hypothetical close-packed volume, but rather as an intensive variable analogous to a temperature. For example, Mehta and Edwards [27] have introduced an intensive variable, thermodynamically conjugate to volume, which must govern density fluctuations in relations such as Eq. (1.3) or (3.1) in much the same way as ordinary temperature governs energy fluctuations. Recently Shi and Falk [28,29] have shown that while the interior of a shear bands in molecular-dynamics simulations has a high density of active STZ's, the actual density in that region is negligibly lower than in the rest of the system, but measurable structural disordering occurs in the shear band that leads to softening.

The idea that $\chi \equiv v_f / V^*$ in Eq. (1.3) might more generally be interpreted as an effective temperature seems especially appealing in light of our argument that the limiting steady-state value of Λ (or equivalently n_∞ or n_{eq}) should depend upon the order in which we take the limits $T \to 0$ and $\dot{\epsilon}^{pl} \to 0$. More realistically, under steady-state conditions, χ might approach some nonzero limiting value and remain there for indefinitely long times at sufficiently small T and for arbitrarily small but nonzero $\dot{\epsilon}^{pl}$. Conversely, χ (in suitable units) might approach the true temperature at large enough T or small enough $\dot{\epsilon}^{pl}$.

There is increasing evidence that something like this happens in sheared foams or granular materials [30–33]. In those systems, the usual kinetic temperature is zero because the constituents have very large masses, but an effective temperature determined by response-fluctuation relations goes to a nonzero limit when the deformation rate becomes arbitrarily small. In our present system, there is a true kinetic temperature, but below the glass transition that temperature is so small that thermally assisted molecular rearrangements are effectively frozen out. During irreversible processes such as plastic deformation therefore the slow, configurational degrees of freedom characterized by χ might fall out of equilibrium with the fast, thermal (vibrational) degrees of freedom, and each may accurately be described by its own "temperature." We suspect that some such description of our system will be necessary in order to resolve the two-limit problem that we have encountered here.

[1] J. S. Langer and L. Pechenik, Phys. Rev. E **68**, 061507 (2003).

[2] D. Turnbull and M. Cohen, J. Chem. Phys. **52**, 3038 (1970).

[3] F. Spaepen, Acta Metall. **25** (4), 407 (1977).

[4] F. Spaepen and A. Taub, in *Physics of Defects*, edited by R. Balian and M. Kleman, 1981 Les Houches Lectures (North-Holland, Amsterdam, 1981), p. 133.

[5] A. S. Argon and L. T. Shi, Acta Metall. **31**, 499 (1983).

[6] D. Srolovitz, K. Maeda, V. Vitek, and T. Egami, Philos. Mag. A **44**, 847 (1981).

[7] D. Deng, A. S. Argon, and S. Yip, Philos. Trans. R. Soc. London, Ser. A **329**, 549 (1989).

[8] A. S. Krausz and H. Eyring, *Deformation Kinetics* (Wiley, New York, 1975).

[9] P. De Hey, J. Sietsma, and A. Van Den Beukel, Acta Mater. **46**, 5873 (1998).

[10] M. L. Falk and J. S. Langer, Phys. Rev. E **57**, 7192 (1998).

[11] W. L. Johnson, J. Lu, and M. D. Demetriou, Intermetallics **10**(11-12), 1039 (2002).

[12] H. Kato, Y. Kawamura, A. Inoue, and H. S. Chen, Appl. Phys. Lett. **73**, 3665 (1998).

[13] J. Lu, G. Ravichandran, and W. L. Johnson, Acta Mater. **51**, 3429 (2003).

[14] L. O. Eastgate, J. S. Langer, and L. Pechenik, Phys. Rev. Lett. **90**, 045506 (2003).

[15] M. L. Falk, Ph.D. thesis, University of California, Santa Barbara, 1998.

[16] L. Pechenik, e-print cond-mat/0305516.

[17] J. S. Langer, Phys. Rev. E **64**, 011504 (2001).

[18] M. L. Falk and J. S. Langer, MRS Bull. **25**, 40 (2000)

[19] M. H. Cohen and G. S. Grest, Phys. Rev. B **20**, 1077 (1979).

[20] A. Masuhr, T. A. Waniuk, R. Busch, and W. L. Johnson, Phys. Rev. Lett. **82**, 2290 (1999).

[21] A. Taub and F. Spaepen, Acta Metall. **28**, 1781 (1980).

[22] A. Greer and F. Spaepen, Ann. N.Y. Acad. Sci. **371**, 218 (1981).

[23] S. Tsao and F. Spaepen, Acta Metall. **33**, 881 (1985).

[24] P. A. Duine, J. Sietsma, and A. van den Beukel, Acta Metall. Mater. **40**, 743 (1992).

[25] O. A. Hasan and M. C. Boyce, Polymer **34**, 5085 (1993).

[26] O. A. Hasan and M. C. Boyce, Polym. Eng. Sci. **34**, 331 (1995).

[27] A. Mehta and S. F. Edwards, Physica A **157**, 1091 (1990).

[28] M. L. Falk, Y. Shi, in *Supercooled Liquids, Glass Transition, and Bulk Metallic Glasses*, edited by T. Egami, A. L. Greer, A. Inoue, and S. Ranganathan, Mater. Res. Soc. Symp. Proc. No. 754 (Materials Research Society, Pittsburgh, PA, 2003), CC6.20.1-6.

[29] Y. Shi and M. L. Falk, submitted to Nat. Mater.

[30] I. K. Ono, C. S. O'Hern, D. J. Durian, S. A. Langer, A. J. Liu, and S. R. Nagel, Phys. Rev. Lett. **89**, 095703 (2002).

[31] L. F. Cugliandolo, J. Kurchan, and L. Peliti, Phys. Rev. E **55**, 3898 (1997).

[32] P. Sollich, F. Lequeux, P. Hebraud, and M. E. Cates, Phys. Rev. Lett. **78**, 2020 (1997).

[33] L. Berthier and J.-L. Barrat, Phys. Rev. Lett. **89**, 095702 (2002).